

Orbital Pumping Incorporating Both Orbital Angular Momentum and Position

Seungyun Han^{**},¹ Hye-Won Ko^{**},² Jung Hyun Oh,² Hyun-Woo Lee,^{1,*} Kyung-Jin Lee,^{2,†} and Kyoung-Whan Kim^{3,4,‡}

¹Department of Physics, Pohang University of Science and Technology, Pohang 37673, Korea

²Department of Physics, Korea Advanced Institute of Science and Technology, Daejeon 34141, Korea

³Department of Physics, Yonsei University, Seoul 03722, Korea

⁴Center for Spintronics, Korea Institute of Science and Technology, Seoul 02792, Korea

We develop a theory of adiabatic orbital pumping, highlighting qualitative differences from spin pumping. An oscillating magnetic field pumps not only orbital angular momentum current but also orbital angular position current. The latter, which has no spin counterpart, underscores the incompleteness of existing orbital torque theories. Importantly, both types of orbital currents can be detected as transverse electric voltages, which contain considerable second harmonic components unlike in spin pumping. Moreover, orbital currents can be pumped by lattice dynamics that carry phonon angular momentum, implying that orbital currents can, in turn, induce phonon angular momentum. Our work opens up new possibilities for generating orbital currents and provides a broader understanding of the interplay between spin, orbital, and phonon dynamics.

Introduction.—Orbital dynamics [1, 2] in solids has recently attracted considerable interest due to its potential to enhance the functionalities of spintronic devices by exploiting the orbital angular momentum of electrons. Phenomena such as the orbital Hall effect [3–12], orbital Edelstein effect [13–15], orbital magnetoresistance [16, 17], and orbital torque [18–23] could, respectively, complement and strengthen the functionalities achieved by the spin Hall effect [24, 25], spin Edelstein effect [26, 27], spin magnetoresistance [28], and spin torque [29, 30]. Moreover, stronger orbital-related phenomena than spin-related ones in a wider class of materials [9, 14, 15] open the field of orbitronics.

Despite recent progress, the fundamental understanding of orbital dynamics lags far behind that of spin dynamics. Advancing orbitronics requires identifying qualitative differences between orbital and spin dynamics. In this regard, we note that orbitals have more degrees of freedom than spin. Whereas three spin operators (S_x, S_y, S_z) completely describe spin 1/2 states, three orbital angular momentum (OAM) operators (L_x, L_y, L_z) are insufficient for describing general orbital states because the size of density matrix for orbital is larger than that of spin. For instance, the orbital direction ϕ of the real p -orbital state $\cos \phi |p_x\rangle + \sin \phi |p_y\rangle$ cannot be specified from its expectation values of the OAM operators, which are zero. This necessitates additional orbital operators, called orbital angular position (OAP) operators [31], defined by symmetric combinations of the OAM operators for p orbitals [31]. Whereas the OAM has many properties in common with spin, the OAP does not have any spin counterpart. Thus, the OAP may hold the key for the further development of orbitronics beyond spintronics. A specific Hall response of the OAP was theoretically predicted [31], i.e., the orbital-torsion Hall effect that refers to the OAP-dependent transverse electron flow caused by an electric field. However, the broader responses of OAP and their implications to orbitronics remain poorly understood.

Adiabatic pumping [32] provides critical insights into fundamental dynamics [33]. Adiabatic spin pumping has significantly advanced our understanding of magnetic damping enhancement [34], spin motive force [35–39], and spin torque [40]. Similarly, adiabatic orbital pumping (or orbital

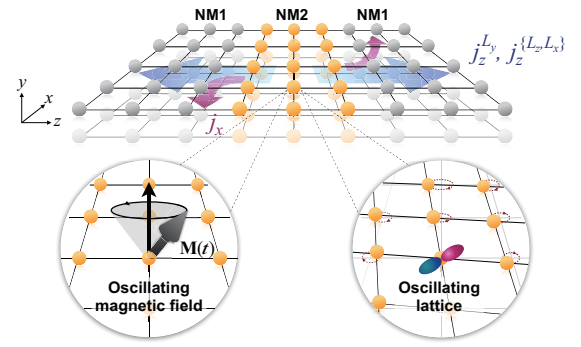


FIG. 1. Schematic illustration of orbital pumping in a model system, NM1/NM2/NM1 (NM = normal metal), driven by an oscillating magnetic field or vibrating lattice. For the magnetic-field-driven case, NM2 may be considered a ferromagnet. j_z^i is an orbital current flowing along z with orbital i , and j_x is a charge current flowing along x .

pumping in short) offers a powerful means to explore the fundamentals of orbital dynamics. However, recent studies on orbital pumping [41–43] have been limited to OAM and have primarily focused on similarities to spin pumping, leaving key differences unexplored.

In this Letter, we present a theory of orbital pumping that incorporates both OAM and OAP degrees of freedom. Our first main finding is that an oscillating magnetic field applied to a ferromagnet (FM) or normal metal (NM) pumps both OAM and OAP currents into neighboring materials (Fig. 1). Onsager reciprocity suggests that orbital torque can be generated in FM not only by OAM injection but also by OAP injection (via orbital-torsion Hall effect [31]). The latter mechanism for generating orbital torque has not been considered in current theories [18, 44] and may demand a re-examination of previous orbital torque experiments [19–23]. Our second finding is that OAM and OAP currents can also be pumped by lattice dynamics carrying phonon angular momentum (PAM). Onsager reciprocity implies that PAM can be excited by injecting electron orbital currents, even in non-chiral materials. Considering recent interest in PAM [45, 46], this finding will stimulate further

studies on the connection between electron's orbital and PAM. It in turn necessitates studies on electron-phonon interaction to include orbital information transfer to phonons. Additionally, we show that orbital pumping generates a second-harmonic response, even in minimally nonlinear situations, which contrasts with the DC and first-harmonic signals produced by spin pumping. This offers a clear experimental method to *qualitatively* distinguish the orbital dynamics from the spin dynamics, providing a means to address the ongoing debate whether existing measurements of orbital relaxation might have actually measured spin relaxation [47].

Orbital pumping by oscillating magnetic field.— In a FM, the perturbation $\mathcal{H}(t) = J_{\text{ex}} \mathbf{L} \cdot \mathbf{M}(t)$ may induce orbital pumping, where \mathbf{L} is the (dimensionless) OAM operator, J_{ex} is the coupling strength, and $\mathbf{M}(t)$ is the unit vector along the magnetization, whose direction is controlled by a magnetic field. Alternatively, orbital pumping may occur from a NM (Fig. 1) when the field couples directly to \mathbf{L} . In this case, $\mathbf{M}(t)$ in $\mathcal{H}(t)$ may be interpreted as the unit vector along the field direction. We ignore the spin degree of freedom to focus solely on orbital responses. To get a tractable analytic formula, we consider a p -orbital system as a minimal model and adopt the atom-center approximation, treating the OAM operator \mathbf{L} as 3×3 matrices in p -orbital space. We also assume an ideal case where three p -orbitals are degenerate in equilibrium. This ideal case reveals critical qualitative differences between orbital pumping and spin pumping. As shown later, our numerical calculations confirm that the predictions from this ideal case persist in real situations, where the p -orbital degeneracy is lifted. We construct a model system of NM1/NM2/NM1 structure (Fig. 1) and derive orbital pumping currents induced by time-dependent perturbations to NM2, where J_{ex} in $\mathcal{H}(t)$ is finite. The 3×3 matrix Green's function g provides a complete description of single-particle dynamics. We abbreviate the explicit position dependence of g for simplicity. For a degenerate p -orbital system, the $\mathbf{L} \cdot \mathbf{M}(t)$ is conserved and g is expanded as $g = \sum_{m=-1,0,1} g_m P_m(t)$, where g_m and $P_m(t) = |\mathbf{L} \cdot \mathbf{M}(t) = m\rangle \langle \mathbf{L} \cdot \mathbf{M}(t) = m|$ are, respectively, the Green's function and projection operator associated with an OAM eigenstate having an eigenvalue m of $\mathbf{L} \cdot \mathbf{M}(t)$.

The pumped current j_α , flowing along the direction α , is given by a 3×3 matrix, similarly to the 2×2 current for spin pumping [34]. Thus, j_α may be expanded in terms of the OAM and OAP as follows,

$$j_\alpha / (-e) = \mathbf{j}_\alpha^{\text{OAM}} \cdot \mathbf{L} + \sum_{\beta\gamma} j_{\alpha,\beta\gamma}^{\text{OAP}} \{L_\beta, L_\gamma\}, \quad (1)$$

since the three 3×3 OAM operators L_x, L_y, L_z and the six 3×3 OAP operators $\{L_\beta, L_\gamma\}$ form a complete set of basis for general 3×3 hermitian matrices [31]. Here $\mathbf{j}_\alpha^{\text{OAM}}$ and $j_{\alpha,\beta\gamma}^{\text{OAP}}$ amount to the pumped OAM and OAP currents, respectively, flowing along α direction. Thus, the complete description of the orbital degrees of freedom naturally leads to the prediction that not only OAM but also OAP are pumped, which is our first main finding. Employing the method developed in Ref. [39],

we obtain

$$\mathbf{j}_\alpha^{\text{OAM}} = \frac{1}{4\pi} \text{Re} \left[\left(\frac{G_\alpha^{1,0} + G_\alpha^{0,-1}}{2} \right) \left(\mathbf{M} \times \frac{d\mathbf{M}}{dt} - i \frac{d\mathbf{M}}{dt} \right) \right], \quad (2)$$

$$j_{\alpha,\beta\gamma}^{\text{OAP}} = \frac{1}{8\pi} \text{Re} \left[\left(\frac{G_\alpha^{1,0} - G_\alpha^{0,-1}}{2} \right) \times \left(M_\beta \left(\mathbf{M} \times \frac{d\mathbf{M}}{dt} \right)_\gamma - i M_\beta \frac{dM_\gamma}{dt} + (\beta \leftrightarrow \gamma) \right) \right] \quad (3)$$

where

$$G_\alpha^{\mu,\nu} = \frac{J_{\text{ex}} \hbar^2}{m_e} \int dr' [g_\mu^R(r, r') \overset{\leftrightarrow}{\partial}_\alpha g_\nu^A(r', r)], \quad (4)$$

which is the orbital-generalization of the spin-mixing conductance for the spin pumping [34]. Here, $g^{R/A}$ represents retarded/advanced Green's function of the NM1/NM2/NM1 heterostructure, $\overset{\leftrightarrow}{\partial}_\alpha$ is the antisymmetric differential operator, and $\int dr'$ denotes the volume integral.

To investigate implications of Eqs. (2) and (3), we consider a specific situation in Fig. 1, where $\alpha = z$ is the pumping direction. When $\mathbf{M}(t)$ rotates in the zx plane ($\mathbf{M}(t) = \hat{z} \cos \omega t + \hat{x} \sin \omega t$), $j_z^{\text{OAM}} = \mathbf{j}_z^{\text{OAM}} \cdot \mathbf{L}$ and $j_z^{\text{OAP}} = \sum_{\beta\gamma} j_{z,\beta\gamma}^{\text{OAP}} \{L_\beta, L_\gamma\}$ become

$$j_z^{\text{OAM}} = \frac{\omega}{4\pi} \left\{ \text{Re}[G_L^+] L_y + \text{Im}[G_L^+] (L_x \cos \omega t - L_z \sin \omega t) \right\}, \quad (5)$$

$$j_z^{\text{OAP}} = \frac{\omega}{4\pi} \text{Im}[G_L^-] \left(\{L_z, L_x\} \cos 2\omega t - (L_z^2 - L_x^2) \sin 2\omega t \right) + \frac{\omega}{4\pi} \text{Re}[G_L^-] \left(\{L_y, L_z\} \cos \omega t + \{L_x, L_y\} \sin \omega t \right), \quad (6)$$

where $G_L^\pm = (G_z^{1,0} \pm G_z^{0,-1})/2$. Here, j_z^{OAM} and j_z^{OAP} are the operator expressions of OAM and OAP currents, respectively. According to Eq. (5), the OAM pumping consists of a DC component carrying L_y and first-harmonic (ω) ones carrying L_x, L_z , which is analogous to the spin pumping. On the other hand, the OAP pumping [Eq. (6)] consists of the first-harmonic components carrying $\{L_y, L_z\}, \{L_x, L_y\}$ and the *second*-harmonic (2ω) ones carrying $\{L_z, L_x\}$ and $L_z^2 - L_x^2$. This difference may be utilized to distinguish the orbital pumping from the spin pumping. As a side remark, the second-harmonic signal generated by orbital pumping is a linear response, which is conceptually different from nonlinear phenomena like the Suhl instability [48–50], and thus experimentally distinguishable.

Next, we numerically examine orbital pumping in a more realistic situation in the sense that the degeneracy of three p -orbitals is lifted by crystal fields. We adopt a sp^3 tight-binding model in a simple cubic lattice with nearest-neighbor hopping. We assume that all energy bands near the Fermi energy have p -character, so the model describes a p -orbital system. Still, the introduction of an s -character band located above the Fermi energy allows for the generalization of the model to a more realistic situation, where real orbital eigenstates vary with crystal

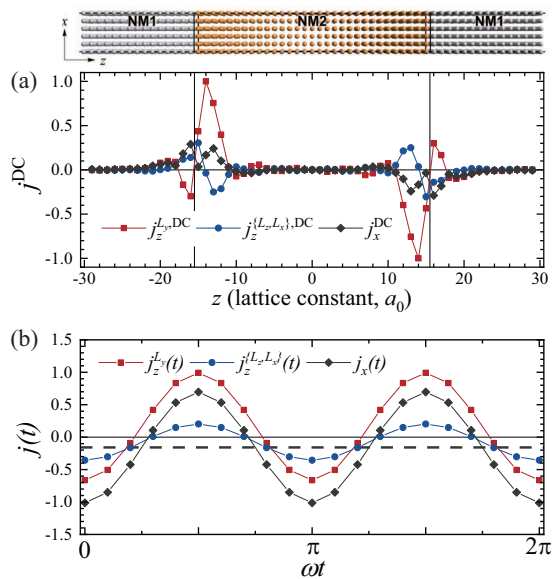


FIG. 2. (a) Spatial profile of DC pumping currents, $j_z^{L_y,DC}$ (red), $j_z^{L_z, L_x, DC}$ (blue), and j_x^{DC} (gray), driven by the time-dependent magnetic field, $\mathbf{L} \cdot \mathbf{M}(t)$ for $\mathbf{M}(t) = \hat{z} \cos \omega t + \hat{x} \sin \omega t$, on NM2 layer. (b) Temporal dependence of pumping currents $j(t)$ at the right interface ($z = 16 a_0$). The thick dashed horizontal line in (b) shows the DC component of transverse charge current $j_x(t)$.

momentum (orbital texture) through sp hybridization [16, 51]. See [52] for further details of the model.

For the same $\mathbf{M}(t)$ given above, we calculate numerically the pumped orbital current using the linear response theory in the adiabatic limit (see [52]). The calculation confirms that all of the orbital currents predicted by Eqs. (5) and (6) are pumped by the $\mathbf{M}(t)$ oscillation. Figure 2 presents some of the numerical results: DC OAM current ($j_z^{L_y,DC}$) [Fig. 2(a)] and second-harmonic OAP current ($j_z^{L_z, L_x}(t)$) [Fig. 2(b)]. It is worth mentioning that OAP pumping currents are comparable in magnitude to OAM pumping currents (Fig. 2). Onsager reciprocity then implies that the orbital torque by OAP injection may be comparable to the conventional orbital torque by OAM injection. In addition, we find pumping of orbital currents that are absent in Eqs. (5) and (6). For instance, the OAM (OAP) current has an unexpected second-harmonic (DC) component [Fig. 2(b)]. This is a result of the inclusion of the crystal field splitting, which can convert OAM current to OAP current and vice versa [31].

In addition to the interconversion between OAM and OAP, we find *intraconversion* among OAM components and *intraconversion* among OAP components, which can be called OAM and OAP swapping effects, respectively (see [52] for details). The OAM swapping effect is analogous to the spin swapping effect [53–55], in line with a recent theory [56]. The OAP swapping effect, however, does not have any spin counterpart. The OAM and OAP swapping effects require the orbital texture but do not require the spin-orbit coupling.

The short decay length (≤ 1 nm) of orbital currents in

NM1 [Fig. 2(a)] is consistent with recent theoretical calculations [47, 57, 58], but much shorter than experimental values (5 ~ 100 nm) [12, 21, 59, 60]. Possible reasons for this discrepancy include disorder scattering [61, 62], multi-grain effects [63, 64], and electron-phonon scattering [60], all of which go beyond the scope of this paper. We argue that this controversy does not affect the predicted qualitative features. In particular, even if the orbital relaxation length is very short, the pumped OAM and OAP currents can be electrically measured through their conversion to transverse charge currents [Fig. 2(a)] via the inverse orbital Hall effect [31, 65, 66] and the inverse orbital-torsion Hall effect [31], respectively, just as pumped spin currents are electrically measured even when their decay length is very short (~ 1 nm) in materials with strong SOC.

A recent orbital pumping experiment [42] reported a DC charge current and attributed it entirely to conversion from pumped DC OAM current [43]. However, according to our calculation, the measured DC charge current contains an additional contribution due to conversion from a pumped DC OAP current. The converted charge current also contains a second-harmonic component since pumped OAM and OAP currents contain second-harmonic components [Fig. 2(b)]. The second-harmonic charge current remains unexplored experimentally. It is worth noting that the generalized pumping equation derived in Supplemental Materials (SM) [52] indicates that a d -orbital system may also produce a fourth-harmonic component. As a spin pumping current contains only DC and first-harmonic components [34], higher-harmonics pumping signals are a unique feature of orbital pumping.

Orbital pumping by lattice dynamics.— Next, we explore orbital pumping due to lattice dynamics, which can be realized by a slowly time-varying strain. The resulting adiabatic variation of a crystal may cause: variations of i) bonding lengths and ii) bonding angles. Each variation manifests in the tight-binding model as corrections to hopping integrals and directional cosines, respectively. The hopping integrals are assumed to follow a power law of bonding length [67, 68]. We integrate the lattice dynamics driven by adiabatically varying strains into our model and numerically calculate the resulting orbital pumping (see SM [52] for details).

We consider a biaxial strain applied to the NM2 layer in our NM1/NM2/NM1 trilayer system (Fig. 1). The biaxial principal axes of the strain are assumed to rotate slowly in the zx plane, which makes our sp -implemented cubic lattice undergo a circularly rotating deformation. This situation mimics the excitation of a long-wavelength phonon vibration with PAM. Numerical calculations with the time-dependent hopping integrals show that both DC OAM current $j_z^{L_y,DC}$ [Fig. 3(a)] and DC OAP current $j_z^{L_z, L_x, DC}$ [Fig. 3(b)] are pumped to the neighboring NM1 layers, and converted to DC transverse charge current j_z^{DC} [Fig. 3(c)]. Thus, the lattice dynamics with PAM generates similar orbital pumping as an oscillating magnetic field does. This is our second main finding, which illustrates a fundamental channel of angular momentum transfer between

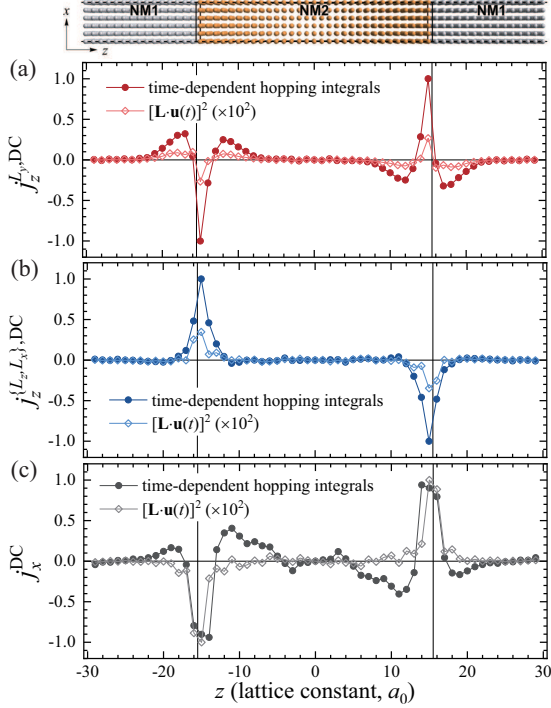


FIG. 3. Spatial profile of DC pumping currents (a) $j_z^{Ly,DC}$, (b) $j_z^{Lz, Lx, DC}$, and (c) j_x^{DC} driven by the lattice dynamics, which is imposed by time-dependent variations of tight-binding hopping integrals (solid circles) and $[\mathbf{L} \cdot \mathbf{u}(t)]^2$ for $\mathbf{u}(t) = \hat{\mathbf{z}} \cos \omega t + \hat{\mathbf{x}} \sin \omega t$ (open diamonds).

electron orbital degrees of freedom and phonons, in addition to the well-known channel between electron spin degree of freedom and magnetization. The OAM pumping induced by the lattice dynamics is the reverse process of crystal field torque [44], where electron OAM, generated by external perturbations such as an electric field, is absorbed by the lattice. Our calculation implies that the reverse process of the OAP current offer an additional mechanism of the crystal field torque that has not been identified before.

To gain an insight, we consider a simplified model focusing on the orbital splitting. Since this perturbation is time-reversal even, the corresponding perturbation Hamiltonian should be expressed in terms of even-order products of the OAM operators, which are OAP operators. To be more specific, we consider a strain applied along the \mathbf{u} direction, and model the resulting perturbation as $K[\mathbf{L} \cdot \mathbf{u}(t)]^2$ where K is the strain-OAP coupling strength (see SM [52]). This modeling is based on the reasoning that the strain tends to make the orbital energy of the p_u orbital different from those of the other p orbitals perpendicular to it. The perturbation $K[\mathbf{L} \cdot \mathbf{u}(t)]^2$ does exactly this job. The open diamonds in Fig. 3 show the orbital currents pumped by the $K[\mathbf{L} \cdot \mathbf{u}(t)]^2$ perturbation incorporated to the numerical model. Note that the results from this simplified model reproduce the characteristics of orbital pumping obtained from the previous numerical calculation that incorporates i) and ii).

We simplify the model further so that analytic calculation

becomes possible. In the limit of the negligible crystal field, the orbital splitting is governed by the perturbation $K[\mathbf{L} \cdot \mathbf{u}(t)]^2$ and the Green's function in the presence of the perturbation can be expressed as $g = g_0 I + (g_1 - g_0)[\mathbf{L} \cdot \mathbf{u}(t)]^2$. Then, we obtain

$$\mathbf{j}_\alpha^{\text{OAM}} = \frac{1}{4\pi} \text{Re}[G_\alpha^{1,0}] \mathbf{u} \times \frac{d\mathbf{u}}{dt}, \quad (7)$$

$$j_{\alpha,\beta\gamma}^{\text{OAP}} = \frac{1}{8\pi} \text{Im}[G_\alpha^{1,0}] \frac{d(u_\beta u_\gamma)}{dt}, \quad (8)$$

where $G_\alpha^{\mu,\nu}$ is given by Eq. (4) except that J_{ex} is replaced by K . We take $\mathbf{u}(t) = \hat{\mathbf{z}} \cos \omega t + \hat{\mathbf{x}} \sin \omega t$ to mimic the adiabatically rotating biaxial strain examined above numerically. Equation (7) then predicts the pumping of the DC OAM current $j_z^{Ly,DC}$, which can be understood as the transfer of PAM to electron OAM [69]. On the other hand, the total derivative in Eq. (8) predicts the pumped OAP current $j_z^{Lz, Lx}(t)$ not to have any DC component. The emergence of DC OAP current $j_z^{Lz, Lx, DC}$ in numerical calculations [Fig. 3(b)] is again attributed to the orbital texture, resulting in an interconversion between OAM and OAP, as generally proven in Ref. [31].

Discussion and outlook.— We demonstrated orbital pumping driven by either oscillating $\mathbf{M}(t)$ or lattice dynamics $\mathbf{u}(t)$. The simultaneous emergence of OAM and OAP pumping for both pumping methods highlights the necessity of considering both orbital degrees of freedom when describing orbital dynamics. This result has an important implication for orbital torque. It has been believed that orbital torque originates solely from the injection of OAM current [18]. However, the pumping of OAP current through magnetization dynamics suggests the existence of its inverse process: the generation of magnetic torque through the injection of OAP current. This previously unrecognized inverse process, which we term ‘‘OAP torque’’, introduces a new dimension to the understanding of orbital torque. For instance, the OAP torque implies that the Onsager reciprocity between orbital pumping and orbital torque is validated only when one considers both OAM and OAP contributions.

Our theory of orbital pumping also offers an exploitable method to generate orbital currents, just as spin pumping serves as an efficient means to generate a pure spin current [70, 71]. Considering that our theory neglects the spin degree of freedom, we expect that orbital magnets may be ideal materials to generate an almost pure orbital current through pumping since their magnetization is dominated by the orbital magnetic moment. Examples include CoMnO_3 films [72]. We note that previous suggestions [31] for the orbital current generation method rely on twisted heterostructures, which can be challenging to implement, or on low-gap semiconductors with limited availability of the required materials. In contrast, the high-harmonics pumping driven by the OAP degree of freedom can be realized with various materials since spin pumping is governed by the DC and first-harmonic components. Thus, orbital pumping extends the scope of orbitronics to a broader range of systems. We also note that this property stems from the distinct behaviors of high-order products of L operators

with respect to rotational transformations. Thus, it is a general property not limited to p -orbital systems.

Furthermore, we argue that orbital pumping is not limited to multilayer structures and may be extended to *single-layer bulk materials*. Recalling that the spin motive force is a continuum version of spin pumping [73] and occurs in single-layer bulk materials, we anticipate the presence of an orbital motive force (continuum version of orbital pumping) when a single-layer system exhibits an inhomogeneous crystal field. Thus, the orbital motive force would encompass OAP contributions, which lack their spin counterparts. Notably, the physical properties of the orbital motive force would differ from those of the spin motive force due to the presence of orbital texture, a factor not accounted for in the theory of the spin motive force. The exploration of this topic remains a subject for future work.

Lastly, our work sheds light on the transfer of angular momentum between electrons and phonons. Theoretical estimations [45, 74, 75] and experimental measurements [46, 76, 77] illustrate that PAM can have a considerable magnitude contrary to early assumptions and plays a nontrivial role in various phenomena such as magnetization relaxation [78] and ultrafast demagnetization [79, 80]. Intriguingly, recent many-body treatment [81] shows that a complete picture of angular momentum transfer between electron and phonon subsystems requires OAM as a key ingredient since the electron-phonon coupling is independent of spin. The strain-induced orbital pumping weighs heavily on this connection of orbital and lattice and call for a wider viewpoint on PAM dynamics [69, 82–85] assisted by the orbital degree of freedom [86].

H.-W.L. acknowledges Antonio Azevedo for the fruitful discussion. This work was supported by the National Research Foundation of Korea (NRF) funded by the Ministry of Science and ICT (2020R1A2C3013302, 2022M3I7A2079267, RS-2024-00334933, RS-2024-00410027) and the KIST Institutional Program. S.H. and H.-W.L. were supported by the Samsung Science and Technology Foundation (BA-1501-51).

**S.H. and H.-W.K. contributed equally to this work.

* hwl@postech.ac.kr

† kjlee@kaist.ac.kr

‡ kwkim@yonsei.ac.kr

- [1] D. Go, D. Jo, H.-W. Lee, M. Kläui, and Y. Mokrousov, Orbitronics: Orbital currents in solids, *Europhys. Lett.* **135**, 37001 (2021).
- [2] D. Jo, D. Go, G.-M. Choi, and H.-W. Lee, Spintronics meets orbitronics: Emergence of orbital angular momentum in solids, *npj Spintronics* **2**, 19 (2024).
- [3] B. A. Bernevig, T. L. Hughes, and S.-C. Zhang, Orbitronics: The Intrinsic Orbital Current in p -Doped Silicon, *Phys. Rev. Lett.* **95**, 066601 (2005).
- [4] T. Tanaka, H. Kontani, M. Naito, T. Naito, D. S. Hirashima, K. Yamada, and J. Inoue, Intrinsic spin Hall effect and orbital Hall effect in $4d$ and $5d$ transition metals, *Phys. Rev. B* **77**, 165117 (2008).
- [5] H. Kontani, T. Tanaka, D. S. Hirashima, K. Yamada, and J. Inoue, Giant Intrinsic Spin and Orbital Hall Effects in Sr_2MO_4 ($M = \text{Ru}, \text{Rh}, \text{Mo}$), *Phys. Rev. Lett.* **100**, 096601 (2008).
- [6] H. Kontani, T. Tanaka, D. S. Hirashima, K. Yamada, and J. Inoue, Giant Orbital Hall Effect in Transition Metals: Origin of Large Spin and Anomalous Hall Effects, *Phys. Rev. Lett.* **102**, 016601 (2009).
- [7] I. V. Tokatly, Orbital momentum Hall effect in p -doped graphene, *Phys. Rev. B* **82**, 161404(R) (2010).
- [8] D. Go, D. Jo, C. Kim, and H.-W. Lee, Intrinsic Spin and Orbital Hall Effects from Orbital Texture, *Phys. Rev. Lett.* **121**, 086602 (2018).
- [9] D. Jo, D. Go, and H.-W. Lee, Gigantic intrinsic orbital Hall effects in weakly spin-orbit coupled metals, *Phys. Rev. B* **98**, 214405 (2018).
- [10] S. Bhowal and G. Vignale, Orbital Hall effect as an alternative to valley Hall effect in gapped graphene, *Phys. Rev. B* **103**, 195309 (2021).
- [11] T. P. Cysne, M. Costa, L. M. Canonico, M. B. Nardelli, R. Muniz, and T. G. Rappoport, Disentangling Orbital and Valley Hall Effects in Bilayers of Transition Metal Dichalcogenides, *Phys. Rev. Lett.* **126**, 056601 (2021).
- [12] Y.-G. Choi, D. Jo, K.-H. Ko, D. Go, K.-H. Kim, H. G. Park, C. Kim, B.-C. Min, G.-M. Choi, and H.-W. Lee, Observation of the orbital Hall effect in a light metal Ti, *Nature* **619**, 52 (2023).
- [13] D. Go, J.-P. Hanke, P. M. Buhl, F. Freimuth, G. Bihlmayer, H.-W. Lee, Y. Mokrousov, and S. Blügel, Toward surface orbitronics: giant orbital magnetism from the orbital Rashba effect at the surface of sp -metals, *Sci. Rep.* **7**, 46742 (2017).
- [14] A. Johansson, B. Göbel, J. Henk, M. Bibes, and I. Mertig, Spin and orbital Edelstein effects in a two-dimensional electron gas: Theory and application to SrTiO_3 interfaces, *Phys. Rev. Res.* **3**, 013275 (2021).
- [15] A. El Hamdi, J.-Y. Chauleau, M. Boselli, C. Thibault, C. Gorini, A. Smogunov, C. Barreateau, S. Gariglio, J.-M. Triscone, and M. Viret, Observation of the orbital inverse Rashba–Edelstein effect, *Nat. Phys.* **19**, 1855 (2023).
- [16] H.-W. Ko, H.-J. Park, G. Go, J. H. Oh, K.-W. Kim, and K.-J. Lee, Role of orbital hybridization in anisotropic magnetoresistance, *Phys. Rev. B* **101**, 184413 (2020).
- [17] S. Ding, Z. Liang, D. Go, C. Yun, M. Xue, Z. Liu, S. Becker, W. Yang, H. Du, C. Wang, Y. Yang, G. Jakob, M. Kläui, Y. Mokrousov, and J. Yang, Observation of the Orbital Rashba–Edelstein Magnetoresistance, *Phys. Rev. Lett.* **128**, 067201 (2022).
- [18] D. Go and H.-W. Lee, Orbital torque: Torque generation by orbital current injection, *Phys. Rev. Res.* **2**, 013177 (2020).
- [19] Z. C. Zheng, Q. X. Guo, D. Jo, D. Go, L. H. Wang, H. C. Chen, W. Yin, X. M. Wang, G. H. Yu, W. He, H.-W. Lee, J. Teng, and T. Zhu, Magnetization switching driven by current-induced torque from weakly spin-orbit coupled Zr, *Phys. Rev. Res.* **2**, 013127 (2020).
- [20] Y. Tazaki, Y. Kageyama, H. Hayashi, T. Harumoto, T. Gao, J. Shi, and K. Ando, Current-induced torque originating from orbital current, [arXiv:2004.09165](https://arxiv.org/abs/2004.09165) (2020).
- [21] D. Lee, D. Go, H.-J. Park, W. Jeong, H.-W. Ko, D. Yun, D. Jo, S. Lee, G. Go, J. H. Oh, K.-J. Kim, B.-G. Park, B.-C. Min, H. C. Koo, H.-W. Lee, O. Lee, and K.-J. Lee, Orbital torque in magnetic bilayers, *Nat. Commun.* **12**, 6710 (2021).
- [22] J. Kim, D. Go, H. Tsai, D. Jo, K. Kondou, H.-W. Lee, and Y. Otani, Nontrivial torque generation by orbital angular momentum injection in ferromagnetic-metal/Cu/Al₂O₃ trilayers, *Phys. Rev. B* **103**, L020407 (2021).
- [23] G. Sala and P. Gambardella, Giant orbital Hall effect and orbital-to-spin conversion in $3d$, $5d$, and $4f$ metallic heterostructures,

- Phys. Rev. Res. **4**, 033037 (2022).
- [24] J. Sinova, D. Culcer, Q. Niu, N. Sinitsyn, T. Jungwirth, and A. H. MacDonald, Universal Intrinsic Spin Hall Effect, Phys. Rev. Lett. **92**, 126603 (2004).
- [25] J. Sinova, S. O. Valenzuela, J. Wunderlich, C. H. Back, and T. Jungwirth, Spin Hall effects, Rev. Mod. Phys. **87**, 1213 (2015).
- [26] V. M. Edelstein, Spin polarization of conduction electrons induced by electric current in two-dimensional asymmetric electron systems, Solid State Commun. **73**, 233–235 (1990).
- [27] J. C. Rojas Sánchez, L. Vila, G. Desfonds, S. Gambarelli, J. P. Attané, J. M. De Teresa, C. Magén, and A. Fert, Spin-to-charge conversion using Rashba coupling at the interface between non-magnetic materials, Nat. Commun. **4**, 2944 (2013).
- [28] H. Nakayama, Y. Kanno, H. An, T. Tashiro, S. Haku, A. Nomura, and K. Ando, Rashba-Edelstein Magnetoresistance in Metallic Heterostructures, Phys. Rev. Lett. **117**, 116602 (2016).
- [29] J. C. Slonczewski, Current-driven excitation of magnetic multilayers, J. Magn. Magn. Mater. **159**, L1 (1996).
- [30] L. Berger, Emission of spin waves by a magnetic multilayer traversed by a current, Phys. Rev. B **54**, 9353 (1996).
- [31] S. Han, H.-W. Lee, and K.-W. Kim, Orbital Dynamics in Centrosymmetric Systems, Phys. Rev. Lett. **128**, 176601 (2022).
- [32] D. J. Thouless, Quantization of particle transport. Phys. Rev. B **27**, 6083 (1983).
- [33] R. Citro and M. Aidelsburger, Thouless pumping and topology, Nat. Rev. Phys. **5**, 87 (2023).
- [34] Y. Tserkovnyak, A. Brataas, and G. E. W. Bauer, Enhanced Gilbert Damping in Thin Ferromagnetic Films, Phys. Rev. Lett. **88**, 117601 (2002).
- [35] K.-W. Kim, J.-H. Moon, K.-J. Lee, and H.-W. Lee, Prediction of Giant Spin Motive Force due to Rashba Spin-Orbit Coupling, Phys. Rev. Lett. **108**, 217202 (2012).
- [36] G. Tatara, N. Nakabayashi, and K.-J. Lee, Spin motive force induced by Rashba interaction in the strong sd coupling regime, Phys. Rev. B **87**, 054403 (2013).
- [37] W. M. Saslow, Spin pumping of current in non-uniform conducting magnets, Phys. Rev. B **76**, 184434 (2007).
- [38] R. Cheng, J. Xiao, Q. Niu, and A. Brataas, Spin Pumping and Spin-Transfer Torques in Antiferromagnets, Phys. Rev. Lett. **113**, 057601 (2014).
- [39] K. Chen and S. Zhang, Spin Pumping in the Presence of Spin-Orbit Coupling, Phys. Rev. Lett. **114**, 126602 (2015).
- [40] Y. Tserkovnyak, A. Brataas, G. E. W. Bauer, and B. I. Halperin, Nonlocal magnetization dynamics in ferromagnetic heterostructures, Rev. Mod. Phys. **77**, 1375 (2005).
- [41] E. Santos, J.E. Abrão, D. Go, L.K. de Assis, Y. Mokrousov, J.B.S. Mendes, and A. Azevedo, Inverse Orbital Torque via Spin-Orbital Intertwined States, Phys. Rev. Appl. **19**, 014069 (2023).
- [42] H. Hayashi, D. Go, S. Haku, Y. Mokrousov, and K. Ando, Observation of orbital pumping, Nat. Electron. **7**, 646 (2024).
- [43] D. Go, K. Ando, A. Pezo, S. Blügel, A. Manchon, and Y. Mokrousov, Orbital Pumping by Magnetization Dynamics in Ferromagnets, arXiv:2309.14817 (2023).
- [44] D. Go, F. Freimuth, J.-P. Hanke, F. Xue, O. Gomonay, K.-J. Lee, S. Blügel, P. M. Haney, H.-W. Lee, and Y. Mokrousov, Theory of current-induced angular momentum transfer dynamics in spin-orbit coupled systems, Phys. Rev. Res. **2**, 033401 (2020).
- [45] L. Zhang and Q. Niu, Angular Momentum of Phonons and the Einstein-de Haas Effect, Phys. Rev. Lett. **112**, 085503 (2014).
- [46] H. Zhu, J. Yi, M.-Y. Li, J. Xiao, L. Zhang, C.-W. Yang, R. A. Kaindl, L.-J. Li, Y. Wang, and X. Zhang, Observation of chiral phonons, Science **359**, 579 (2018).
- [47] M. Rang and P. J. Kelly, Orbital relaxation length from first-principles scattering calculations, Phys. Rev. B **109**, 214427 (2024).
- [48] P. W. Anderson and H. Suhl, Instability in the Motion of Ferromagnets at High Microwave Power Levels, Phys. Rev. **100**, 1788 (1955).
- [49] H. Suhl, The theory of ferromagnetic resonance at high signal powers, J. Phys. Chem. Solids **1**, 209 (1957).
- [50] H. Suhl, Origin and Use of Instabilities in Ferromagnetic Resonance, J. Appl. Phys. **29**, 416 (1958).
- [51] S. Han, H.-W. Lee, and K.-W. Kim, Microscopic study of orbital textures, Curr. Appl. Phys. **50**, 13 (2023).
- [52] See Supplemental Materials for details.
- [53] M. B. Lifshits and M. I. Dyakonov, Swapping Spin Currents: Interchanging Spin and Flow Directions, Phys. Rev. Lett. **103**, 186601 (2009).
- [54] S. Sadjina, A. Brataas, and A. G. Mal'shukov, Intrinsic spin swapping, Phys. Rev. B **85**, 115306 (2012).
- [55] H. B. M. Saïdaoui and A. Manchon, Spin-Swapping Transport and Torques in Ultrathin Magnetic Bilayers, Phys. Rev. Lett. **117**, 036601 (2016).
- [56] A. Manchon, A. Pezo, K.-W. Kim, and K.-J. Lee, Orbital diffusion, polarization and swapping in centrosymmetric metals, arXiv:2310.04763 (2023).
- [57] S. Urazhdin, Symmetry constraints on orbital transport in solids, Phys. Rev. B **108**, L180404 (2023).
- [58] K. D. Belashchenko, G. G. Baez Flores, W. Fang, A. A. Kovalev, M. van Schilfgaarde, P. M. Haney, and M. D. Stiles, Breakdown of the drift-diffusion model for transverse spin transport in a disordered Pt film, Phys. Rev. B, **108**, 144433 (2023).
- [59] H. Moriyama, M. Taniguchi, D. Jo, D. Go, N. Soya, H. Hayashi, Y. Mokrousov, H.-W. Lee, and K. Ando, Observation of Long-Range Current-Induced Torque in Ni/Pt Bilayers, Nano Lett. (2024).
- [60] W. Gao, L. Liao, H. Isshiki, J. Kim, D. Go, Y. Mokrousov, K.-J. Lee, and H.-W. Lee, and Y. Otani, Nonlocal Electrical Detection of Reciprocal Orbital Edelstein Effect (2024).
- [61] H. Liu and D. Culcer, Dominance of Extrinsic Scattering Mechanisms in the Orbital Hall Effect: Graphene, Transition Metal Dichalcogenides, and Topological Antiferromagnets, Phys. Rev. Lett. **132**, 186302 (2024).
- [62] J. Sohn, J. M. Lee, and H.-W. Lee, Dyakonov-Perel-like Orbital and Spin Relaxations in Centrosymmetric Systems, Phys. Rev. Lett. **132**, 246301 (2024).
- [63] L. Liao, F. Xue, L. Han, J. Kim, R. Zhang, L. Li, J. Liu, X. Kou, C. Song, F. Pan, and Y. Otani, Efficient orbital torque in polycrystalline ferromagnetic-metal/Ru/Al₂O₃ stacks: Theory and experiment, Phys. Rev. B **105**, 104434 (2022).
- [64] J. C. Idrobo, J. Ruzs, G. Datt, D. Jo, S. Alikhah, D. Muradas, U. Noubme, M. V. Kamalakar, P. M. Oppeneer, Direct observation of nanometer-scale orbital angular momentum accumulation, arXiv:2403.09269 (2024).
- [65] P. Wang, Z. Feng, Y. Yang, D. Zhang, Q. Liu, Z. Xu, Z. Jia, Y. Wu, G. Yu, X. Xu, and Y. Jiang, Inverse orbital Hall effect and orbitronic terahertz emission observed in the materials with weak spin-orbit coupling, npj Quantum Mater. **8**, 28 (2023).
- [66] Y. Xu, F. Zhang, A. Fert, H.-Y. Jaffres, Y. Liu, R. Xu, Y. Jiang, H. Cheng, and W. Zhao, Orbitronics: Light-induced Orbit Currents in Terahertz Emission Experiments, arXiv:2307.03490 (2023).
- [67] S. Froyen and W. A. Harrison, Elementary prediction of linear combination of atomic orbitals matrix elements, Phys. Rev. B **20**, 2420 (1979).
- [68] W. A. Harrison, Electronic Structure and the Properties of Solids (Freeman, San Francisco, 1980).
- [69] D. Yao and S. Murakami, Chiral-phonon-induced current in

- helical crystals, *Phys. Rev. B* **105**, 184412 (2022).
- [70] O. Mosendz, J. E. Pearson, F. Y. Fradin, G. E. W. Bauer, S. D. Bader, and A. Hoffmann, Quantifying Spin Hall Angles from Spin Pumping: Experiments and Theory, *Phys. Rev. Lett.* **104**, 046601 (2010).
- [71] K. Ando, S. Takahashi, J. Ieda, Y. Kajiwara, H. Nakayama, T. Yoshino, K. Harii, Y. Fujikawa, M. Matsuo, S. Maekawa, and E. Saitoh, Inverse spin-Hall effect induced by spin pumping in metallic system. *J. Appl. Phys.* **109**, 103913 (2011).
- [72] H. Koizumi, S. Sharmin, K. Amemiya, M. Suzuki-Sakamaki, J.-i. Inoue, and H. Yanagihara, Experimental evidence of orbital ferrimagnetism in $\text{CoMnO}_3(0001)$ epitaxial thin film, *Phys. Rev. Mater.* **3**, 024404 (2019).
- [73] S. Zhang and S. S.-L. Zhang, Generalization of the Landau-Lifshitz-Gilbert Equation for Conducting Ferromagnets, *Phys. Rev. Lett.* **102**, 086601 (2009).
- [74] L. Zhang and Q. Niu, Chiral Phonons at High-Symmetry Points in Monolayer Hexagonal Lattices, *Phys. Rev. Lett.* **115**, 115502 (2015).
- [75] Y. Ren, C. Xiao, D. Saparov, and Q. Niu, Phonon Magnetic Moment from Electronic Topological Magnetization, *Phys. Rev. Lett.* **127**, 186403 (2021).
- [76] R. Sasaki, Y. Nii, and Y. Onose, Magnetization control by angular momentum transfer from surface acoustic wave to ferromagnetic spin moments, *Nat. Commun.* **12**, 2599 (2021).
- [77] J. Holanda, D. S. Maior, A. Azevedo, and S. M. Rezende, Detecting the phonon spin in magnon-phonon conversion experiments, *Nat. Phys.* **14**, 500 (2018).
- [78] S. Streib, H. Keshtgar, and G. E. W. Bauer, Damping of Magnetization Dynamics by Phonon Pumping, *Phys. Rev. Lett.* **121**, 027202 (2018).
- [79] C. Dornes, Y. Acremann, M. Savoini, M. Kubli, M. J. Neugebauer, E. Abreu, L. Huber, G. Lantz, C. A. F. Vaz, H. Lemke, E. M. Bothschafter, M. Porer, V. Esposito, L. Rettig, M. Buzzi, A. Alberca, Y. W. Windsor, P. Beaud, U. Staub, D. Zhu, S. Song, J. M. Glownia, and S. L. Johnson, The ultrafast Einstein-de Haas effect, *Nature* **565**, 209 (2019).
- [80] S. R. Tauchert, M. Volkov, D. Ehberger, D. Kazenwadel, M. Evers, H. Lange, A. Donges, A. Book, W. Kreuzpaintner, U. Nowak, and P. Baum, Polarized phonons carry angular momentum in ultrafast demagnetization, *Nature* **602**, 73 (2022).
- [81] J. H. Mentink, M. I. Katsnelson, and M. Leshchko, Quantum many-body dynamics of the Einstein-de Haas effect, *Phys. Rev. B* **99**, 064428 (2019).
- [82] M. Hamada and S. Murakami, Conversion between electron spin and microscopic atomic rotation, *Phys. Rev. Res.* **2**, 023275 (2020).
- [83] D. Yao and S. Murakami, Conversion of Chiral Phonons into Magnons in Ferromagnets and Antiferromagnets, *J. Phys. Soc. Jpn.* **93**, 034708 (2024).
- [84] D. M. Juraschek and N. A. Spaldin, Orbital magnetic moments of phonons, *Phys. Rev. Mater.* **3**, 064405 (2019).
- [85] D. M. Juraschek, P. Narang, and N. A. Spaldin, Phono-magnetic analogs to opto-magnetic effects, *Phys. Rev. Res.* **2**, 043035 (2020).
- [86] C. Xiao, Y. Ren, and B. Xiong, Adiabatically induced orbital magnetization, *Phys. Rev. B* **103**, 115432 (2021).